

# Remnant neuromuscular junctions in denervated muscles contribute to functional recovery in delayed peripheral nerve repair

Leyang Li<sup>1</sup>, Hiroyuki Yokoyama<sup>1</sup>, Hidetoshi Kaburagi<sup>1</sup>, Takashi Hirai<sup>1</sup>, Kunikazu Tsuji<sup>2</sup>, Mitsuhiro Enomoto<sup>1,\*</sup>, Yoshiaki Wakabayashi<sup>1</sup>, Atsushi Okawa<sup>1</sup>

<sup>1</sup> Department of Orthopedic and Spinal Surgery, Graduate School, Tokyo Medical and Dental University, Tokyo, Japan

<sup>2</sup> Department of Cartilage Regeneration, Tokyo Medical and Dental University, Tokyo, Japan

**Funding:** This work was supported by the Japan Society for the Promotion of Science KAKENHI (Grants 26462230 [to YM] and 16K10813 [to ME]) and grants from the Japan Student Services Organization (JASSO).

## Abstract

Schwann cell proliferation in peripheral nerve injury (PNI) enhances axonal regeneration compared to central nerve injury. However, even in PNI, long-term nerve damage without repair induces degeneration of neuromuscular junctions (NMJs), and muscle atrophy results in irreversible dysfunction. The peripheral regeneration of motor axons depends on the duration of skeletal muscle denervation. To overcome this difficulty in nerve regeneration, detailed mechanisms should be determined for not only Schwann cells but also NMJ degeneration after PNI and regeneration after nerve repair. Here, we examined motor axon denervation in the tibialis anterior muscle after peroneal nerve transection in thy1-YFP mice and regeneration with nerve reconstruction using allografts. The number of NMJs in the tibialis anterior muscle was maintained up to 4 weeks and then decreased at 6 weeks after injury. In contrast, the number of Schwann cells showed a stepwise decline and then reached a plateau at 6 weeks after injury. For regeneration, we reconstructed the degenerated nerve with an allograft at 4 and 6 weeks after injury, and evaluated functional and histological outcomes for 10 to 12 weeks after grafting. A higher number of pretzel-shaped NMJs in the tibialis anterior muscle and better functional recovery were observed in mice with a 4-week delay in surgery than in those with a 6-week delay. Nerve repair within 4 weeks after PNI is necessary for successful recovery in mice. Prevention of synaptic acetylcholine receptor degeneration may play a key role in peripheral nerve regeneration. All animal experiments were approved by the Institutional Animal Care and Use Committee of Tokyo Medical and Dental University on 5 July 2017, 30 March 2018, and 15 May 2019 (A2017-311C, A2018-297A, and A2019-248A), respectively.

**Key Words:** axon; nerve allograft; nerve regeneration; neurodegeneration; neuromuscular junction; peripheral nerve injury; Schwann cell; skeletal muscle

**Chinese Library Classification No.** R459.9; R364; R605

## Introduction

Peripheral nerve injuries (PNI) result from crush, avulsion, or mangling injuries to the extremities with high-energy trauma. Microsurgical nerve repair techniques have improved, and nerve autografts, allografts, and transfers have been used to reconstruct peripheral nerve gaps for nearly a century (Millesi, 2000; Sakuma et al., 2016). However, many factors affect the recovery after nerve injury. Surgical repair is sometimes delayed for patients with marked deterioration of their general condition. Delayed nerve repair could affect functional recovery (Fu and Gordon, 1995a, b) and give rise to progressive atrophy in denervated muscles due to a lack of electrical and neurotrophic stimulation (Ashley et al., 2007; Jonsson et al., 2013). There is no specific time point by when repair should occur after PNI, although it is generally accepted that early surgical intervention is required for functional recovery (Rosenfield and Paksima, 2001; Susarla et al., 2007; Jivan et al., 2009).

Degeneration of neuromuscular junctions (NMJs) should be considered when repairing injured nerves after PNI (Birks et al., 1960). NMJs are a type of peripheral synapse

that efficiently transmits information from motor nerves to muscle fibers, and they mediate neuronal stimulation to induce muscle contractions. The molecular mechanisms in denervated muscles are not well understood but can be explored using animal experiments (Scheib and Höke, 2013). In a rat experiment, the number of NMJs was maintained for 18 days after transection of the sciatic nerve, and then decreased to 54% of normal after 33 days and 35% of normal after 57 days (Andreose et al., 1995). In mouse experiments, the time window for regeneration was found to be within 35 days after PNI, and differential regulation of matrix metalloproteinase 3 or heat shock protein 27 was needed beyond the critical point (Ma et al., 2011; Chao et al., 2013). Functional recovery was not observed, even though the regenerated nerve reached the target muscles after sciatic nerve crush injury (Sakuma et al., 2016). It is possible that deterioration of the endplate structure could result in nonviable muscles. Therefore, quantitative and qualitative analyses of the NMJs should be performed during degeneration and regeneration in the target muscles after PNI.

B6.Cg-Tg (Thy1-YFP) 16Jrs/J transgenic mice express yellow fluorescent protein (YFP) in motor and sensory neurons

\*Correspondence to:

Mitsuhiro Enomoto, MD, PhD,  
enomorth@tmd.ac.jp.

orcid:

0000-0001-8204-0185  
(Mitsuhiro Enomoto)

doi: 10.4103/1673-5374.266925

Received: June 16, 2019

Peer review started: June 20, 2019

Accepted: August 22, 2019

Published online: October 18, 2019

under control of the mouse Thy1 promoter (Feng et al., 2000; Webb et al., 2012). These mice are useful for visualizing motor axons and end plates in skeletal muscles. Postsynaptic acetylcholine receptors (AChRs) are labeled by  $\alpha$ -bungarotoxin (BTX) in NMJs, and the connections between axons and AChRs are clearly observed in histology (Keller-Peck et al., 2001; Lin et al., 2001). In a PNI model, such mice can be used to observe regenerated axons expressing YFP. In particular, Thy1-YFP mice have been used to calculate the rate of nerve regeneration after saphenous nerve crush (Yan et al., 2011). Such mice can thus be used to obtain a better understanding of the relationship between regenerated axons and NMJs.

In the present study, we conjectured that NMJs might play an important role in nerve regeneration in the chronic phase after PNI. First, we evaluated the degeneration pattern of NMJs in denervated muscles in an animal model of PNI animal. Second, we evaluated whether delayed peripheral nerve grafting resulted in functional recovery under conditions of poor axonal regeneration, and whether never repair within 4 or 6 weeks after PNI was histologically improved. Finally, we discussed how degeneration and regeneration of NMJs were related to motor function after delayed peripheral nerve repair.

## Materials and Methods

### Experimental animals and design

All animal experiments were approved by the Institutional Animal Care and Use Committee of Tokyo Medical and Dental University on 5 July 2017, 30 March 2018, and 15 May 2019 (A2017-311C, A2018-297A, and A2019-248A), respectively. B6.Cg-Tg (Thy1-YFP) 16Jrs/J mice were obtained from Jackson Laboratory (Bar Harbor, ME, USA). One hundred and sixty female 8–10-week-old YFP mice weighting approximately 18 g were kept in standard cages at a constant temperature and light/dark cycle of 12 hours each, with the light/dark hours changing automatically, and given water and food *ad libitum* throughout the experimental period. One week before and during the whole experiment, the mice were housed in a sterile room with an ambient temperature of 25°C to prevent infection and external stimulation. The mice were randomly divided into four experimental groups: naïve control (NC,  $n = 20$ ), surgical control (SC,  $n = 80$ ), and allograft (AG) transplantation at 4 (AG4,  $n = 30$ ) and 6 weeks after injury (AG6 group,  $n = 30$ ). The SC group was divided into eight subgroups randomly at 2, 4, 6, 8, 10, 12, 14, and 16 weeks after transection (each group,  $n = 10$ ). As a donor supply, fresh peroneal nerves of female 8-week-old C57BL/6J mice ( $n = 20$ ) were used in the AG groups.

### Surgical procedure

The mice were anesthetized under 1.5% isoflurane (Forane; Baxter, Deerfield, IL, USA) gas mixture, with 1.5 L/min room air flow. The left peroneal nerve that descended obliquely to the fibula head was fully exposed. Under magnifying lenses (SZ61, Olympus, Tokyo, Japan), the nerve was ligated at approximately 3 mm distant from the tibialis anterior (TA) muscle using 8-0 silk and then the distal stump was excised to denervate the muscle completely. Then, the

skin was sutured with 4-0 monofilament. In the NC group, the nerves were only exposed, and then the muscle layers and skin were closed. We carefully dissected the peroneal nerve away from the soft tissues and ligated the nerve tightly to prevent regeneration from the proximal nerve stump.

To reconstruct the injured peroneal nerve, a 1-mm length of the proximal stump including the ligation thread was resected after exposure of the injured area. A 5-mm segment of donor peroneal nerve from C57BL/6 mice was transplanted to the proximal stump of the injured nerve in an end-to-end manner using a single layer of 8-0 monofilament suture at 4 or 6 weeks after injury. The distal end of the donor nerve was inserted into the TA muscle layer to ensure reinnervation after the anastomosis of the proximal end. All surgeries were performed on the left hindlimb in the surgical group, with the right hindlimb remaining intact as a control. The observation period was 16 weeks in the SC and NC groups, 12 weeks in the AG4 group, and 10 weeks in the AG6 group. This resulted in the same total observation period in the experimental groups.

### Tissue preparation of TA muscles

Tissue analyses were performed at 2, 4, 6, 8, 10, 12, 14 and 16 weeks post-injury in the SC group ( $n = 10$  at each point); at 4 ( $n = 10$ ), 8 ( $n = 10$ ), and 12 weeks ( $n = 10$ ) post-repair in the AG4 group; and at 4 ( $n = 10$ ), 8 ( $n = 10$ ), and 10 weeks ( $n = 10$ ) post-repair in the AG6 group. After the body weight was measured and the hindlimb function was tested, the mice were deeply anesthetized through intraperitoneal injection of 10% pentobarbital sodium in 0.9% physiological saline (0.1 mL/g), and transcardially perfused with a solution of 4% paraformaldehyde in 0.1 M PB (phosphate buffer). The TA muscle and peroneal nerve were carefully dissected from the hindlimbs. The muscles and nerves were post-fixed in 4% paraformaldehyde in 0.1 M PB for 24 hours and dehydrated in 30% sucrose in 0.1 M PB for 48 hours. The tissues were then embedded in 4% carboxymethyl cellulose compound (Finetec Co., Ltd., Tokyo, Japan) and frozen in liquid nitrogen-cooled 2-methylbutane. The tissues were stored at  $-80^{\circ}\text{C}$  until further analysis.

### Immunohistochemistry

Muscles and nerves were cut into 20- $\mu\text{m}$  longitudinal sections using a cryostat, and muscle sections at every 400  $\mu\text{m}$  were used for quantification. Sections from each experimental group were stained with  $\alpha$ -BTX recognized as  $\alpha$ -subunit of AChR of NMJ and/or anti-S100 antibody recognized as myelin-forming Schwann cell. After treatment with 0.2% Triton X-100 for 5 minutes, the TA muscle sections were blocked with 5% normal goat serum (NGS; Vector Laboratories, Burlingame, CA, USA) and incubated with  $\alpha$ -BTX conjugated with Alexa Fluor 594 (1:1000, Invitrogen, Carlsbad, CA, USA) for 1 hour at room temperature and/or rabbit polyclonal anti-S100 (1:300, Novocastra, Newcastle, UK) for 24 hours at 4°C, and the peroneal nerves were incubated with only anti-S100 for 24 hours at 4°C. The S100 antibody was visualized with goat anti-rabbit IgG Alexa 647 (1:300, Invitrogen, Carlsbad, CA, USA) for 1 hour at room temperature. Images were obtained on an AX70 Olympus microscope (Olympus Optical Co., Ltd., Tokyo, Japan).

### Quantitative analyses of NMJs and Schwann cells

To evaluate AChR distribution and Schwann cells quantitatively, sections sampled every 400  $\mu\text{m}$  were stained with  $\alpha$ -BTX and S100, and images were obtained using an AX70 Olympus microscope with 20 $\times$  magnification. We counted  $\alpha$ -BTX-positive clusters and S100-positive fibers in all selected sections for each animal as estimated numbers. We also evaluated the morphology of  $\alpha$ -BTX-positive clusters (Marques et al., 2000; Kummer et al., 2004; Shi et al., 2010; Kurimoto et al., 2016), which was divided into three types: “pretzel” (mature, with a weblike pattern including multiple perforations), “plaque” (immature and smaller size lacking perforations), and “intermediate” (between plaque and pretzel morphology). The positive clusters were counted with regard to the morphology type. The ratio of each type to the total number of  $\alpha$ -BTX-positive clusters was calculated to provide a morphological index for NMJs.

### Functional assessment

We evaluated functional recovery every 2 weeks after transection and grafting using video analysis (Bervar, 2000). For the analyses, each mouse was placed in an acrylic box sized 40 cm  $\times$  7 cm  $\times$  9 cm for acclimation to the testing environment. A video camera was placed 20 cm from the bottom of the apparatus using a ruler. At each time point, the mice were recorded during walking and stopping at a moderate pace over a 5-minute interval. Footprints were measured under static conditions from video images, and the peroneal nerve function index (PFI) was calculated (de Medinaceli et al., 1982; Bain et al., 1989). This index is reliable for measuring functional recovery following peroneal nerve injury compared to the uninjured hindpaw. Toe spread (TS) was measured as the distance between first and fifth toes on the normal side (N) and the contralateral experimental side (E) for the hindpaws of each mouse using ImageJ software (<http://rsb.info.nih.gov/ij/>). The PFI was calculated using the following formula (Inserra et al., 1998):  $\text{PFI} = 191.1[(\text{ETS} - \text{NTS})/\text{NTS}] - 9.86$ .

Unhealed nerve transection was defined as  $-100$  and sham operation was defined as  $0$  (Inserra et al., 1998). The PFI in this experiment had a negative value ( $-97.0 \pm 1.5$ ; 16 weeks after injury), and the value increased to close to  $0$  ( $-4.2 \pm 1.3$ ; naïve mice), indicating functional improvement of the injured peroneal nerves.

Muscle evoked potentials (MEPs) in both hindlimbs induced by electrical stimulation were recorded using an electromyographic device (Neuropack  $\mu$ , Nihon Koden, Tokyo, Japan) at the final observation point under gas anesthesia (1.5% isoflurane gas mixture with 1.5 L/min room air flow). The sciatic nerve was stimulated using a surface electrode (UL2-2020, Unique Medical Co., Ltd., Tokyo, Japan). The stimulus intensity was 0.2 mA, and the duration time was 0.2 ms. MEPs were recorded from the TA muscle. The stimulation was repeated three times, and the acquired amplitude values (measured peak to peak) and terminal latencies of the MEPs were averaged to evaluate the motor function recovery.

### Statistical analysis

All data are expressed as the mean  $\pm$  standard error of the

mean (SEM). The results were analyzed using GraphPad Prism5 statistical software (GraphPad Software Inc., San Diego, CA, USA). Two-way analysis of variance (ANOVA) followed by Bonferroni *post hoc* test was used to compare the values of morphological changes of NMJs after injury in the SC group, and the  $\alpha$ -BTX positive clusters, morphological changes of NMJs, S100-positive fibers, and PFI at every time point among the four groups. Unpaired two-tailed Student's *t*-test was used to compare innervated  $\alpha$ -BTX-positive clusters, terminal latencies, and acquired amplitude values between the AG4 and the AG6 groups. All other analyses utilized one-way ANOVA followed by Tukey's *post hoc* test.  $P < 0.05$  was considered statistically significant.

## Results

### Nerve and NMJ degeneration in TA muscles atrophied by peroneal nerve transection

Table 1 shows the histological evaluations of the muscles of the experimental groups. NMJs and Schwann cells were labeled with  $\alpha$ -BTX and S100, respectively, in the TA muscle (Figure 1A). After transection, YFP-positive axons were not observed in the muscles at 3 days. Loss of  $\alpha$ -BTX and S100 colabeling was observed 14 days after transection. YFP-positive axons were never observed, and severe degeneration of NMJs occurred by 16 weeks after transection.

The number of  $\alpha$ -BTX-positive clusters was counted at each time point (Figure 1B) and decreased up to 16 weeks after transection. The mean number of  $\alpha$ -BTX-positive clusters was temporarily increased at 2 weeks compared to that in the preoperative muscles (pre:  $148.7 \pm 3.0$  vs. 2 weeks:  $166.2 \pm 5.6$  clusters,  $P < 0.01$ ; Figure 1B). Subsequently, the number significantly decreased from 4 weeks ( $163.2 \pm 4.5$  clusters) to 6 weeks ( $101.6 \pm 4.3$  clusters) and 12 weeks ( $19.60 \pm 1.5$  clusters). There was a significant difference between 4 and 6 weeks after transection ( $P < 0.001$ , Figure 1B).

We also analyzed morphological changes of the NMJs after transection. NMJs were divided into three phenotypes (pretzel, intermediate, and plaque) (Figure 1C). The pretzel pattern was predominant in the naïve muscle (pretzel:  $51.7 \pm 2.3\%$ , intermediate:  $31.6 \pm 0.7\%$ , plaque:  $16.7 \pm 2.4\%$ ). The number of plaques increased up to 16 weeks in the denervated muscles and the distribution pattern was changed at 16 weeks (pretzel:  $2.9 \pm 1.2\%$ , intermediate:  $28.8 \pm 2.1\%$ , plaque:  $68.3 \pm 2.1\%$ ). There was no difference in the proportions of the pretzel and plaque types at 6 weeks (Figure 1C). The proportion of the pretzel type at 4 weeks was significantly higher than that at 6 weeks ( $43.7 \pm 1.5\%$  vs.  $36.5 \pm 1.2\%$ ,  $P < 0.05$ ).

We further counted S100-positive areas in the muscles until 16 weeks after transection (Figure 1D). The mean number of S100-positive fibers decreased and reached a plateau at 6 weeks (naïve:  $115.7 \pm 3.3$  fibers vs. 6 weeks:  $23.3 \pm 1.6$  fibers) that was maintained until 16 weeks. The number at 6 weeks was significantly decreased compared to that at 4 weeks after injury ( $23.3 \pm 1.6$  fibers vs.  $41.0 \pm 1.921$  fibers,  $P < 0.001$ ; Figure 1D).

### Nerve regeneration and prevention of NMJ degeneration in TA muscles after nerve grafting

We evaluated the regeneration of YFP axons after allograft

transplantation at the fourth (AG4) and sixth weeks (AG6) after injury, and analyzed the donor nerves with the sutured site and the TA muscles. Donor nerves did not express YFP at 2 weeks, but showed YFP expression at 4 weeks after grafting in both the AG4 (Figure 2A) and AG6 groups (Figure 2B). YFP expression in the TA muscles was increased at the final observation point in both the AG4 and AG6 groups (Figure 2C and D). S100-positive fibers were also observed around the YFP axons.  $\alpha$ -BTX-positive clusters with the pretzel pattern were observed in both groups, but were fragmented in the AG6 group (D2 and D3 in Figure 2D)

#### Alteration of NMJ components after nerve grafting

The number of  $\alpha$ -BTX positive clusters (Figure 3A) in the sections increased after grafting in the AG4 ( $107.8 \pm 4.9$  clusters) and AG6 groups ( $97.5 \pm 5.4$  clusters) 4 weeks after grafting compared to the SC group (8 weeks after transection:  $87.3 \pm 4.4$  clusters, 10 weeks after transection:  $76.7 \pm 4.3$  clusters). At the final observation point, the number of  $\alpha$ -BTX-positive clusters was higher in the AG4 group (12 weeks after grafting:  $70.8 \pm 7.5$  clusters) than in the AG6 (10 weeks after grafting:  $28.6 \pm 5.7$  clusters) and SC groups (16 weeks after transection:  $11.3 \pm 1.2$  clusters).

The frequency of each type of AChRs distribution pattern (i.e., each type of  $\alpha$ -BTX-positive cluster) relative to the total number of  $\alpha$ -BTX-positive clusters was also compared among the groups at the final observation point (Figure 3B). The pretzel type was more prevalent in the AG4 group ( $15.3 \pm 1.6\%$ ) than in the SC ( $2.1 \pm 1.1\%$ ) and AG6 groups ( $5.9 \pm 2.3\%$ ). The intermediate type was more prevalent in the AG6 group ( $43.2 \pm 2.5\%$ ) than in the SC ( $28.8 \pm 2.1\%$ ) and AG4 groups ( $24.9 \pm 1.9\%$ ). The plaque type was more prevalent in the SC group ( $69.1 \pm 1.8\%$ ) than in the AG4 ( $59.8 \pm 2.3\%$ ) and AG6 groups ( $50.8 \pm 1.6\%$ ). The pretzel type persisted in the AG4 group compared to the AG6 group. To elucidate reinnervation with respect to AChRs expression, the number of  $\alpha$ -BTX-positive clusters contacting YFP-positive axons were counted (Figure 3C). At 4 weeks after repair, there was no significant difference in the number of  $\alpha$ -BTX-positive clusters contacting YFP-positive axons between the AG4 and AG6 groups. At the final observation point, all  $\alpha$ -BTX-positive clusters were contacting YFP axons in both the AG4 and AG6 groups, whereas no such contact was observed in the SC group. There was no difference in the number of innervated  $\alpha$ -BTX-positive clusters between the AG4 and AG6 groups.

The number of S100-positive fibers in the TA muscles (Figure 3D) increased in the AG4 group at 4 weeks after grafting ( $48.9 \pm 3.6$  fibers) compared to the SC group at 8 weeks after transection ( $18.1 \pm 1.7$  fibers), and in the AG6 group at 4 weeks after grafting ( $34.8 \pm 2.8$  fibers) compared to the SC group at 10 weeks after transection ( $18.1 \pm 1.9$  fibers). At the final observation point, the number of S100-positive fibers in the AG6 group ( $27.7 \pm 2.7$  fibers) was decreased and similar to that in the SC group ( $18.7 \pm 1.5$  fibers), but the number of S100-positive fibers significantly increased in the AG4 group ( $60.1 \pm 5.9$  fibers).

#### Functional recovery of the hind paw after grafting

The PFI value was  $-4.18 \pm 1.28$  before and decreased to

nearly  $-100$  after transection in the SC group. Grafting times were set at 4 and 6 weeks after transection. There was a significant decrease in PFI value between 4 ( $-57.94 \pm 2.68$ ) and 6 weeks ( $-72.00 \pm 3.43$ ) after transection (Figure 4A).

After grafting, the PFI value was maintained for 6 weeks in both the AG4 and AG6 groups and showed a greater improvement than that in the SC group. The PFI value in the AG4 group increased after grafting, but that in the AG6 group suddenly decreased at 8 weeks after grafting (Figure 4A). The PFI values at the final observation points were  $-96.95 \pm 1.52$ ,  $-41.58 \pm 4.39$ , and  $-86.46 \pm 4.75$  in the SC, AG4, and AG6 groups, respectively. There was a significant increase in the AG4 group compared to the SC and AG6 groups ( $P < 0.001$ , Figure 4A). Video analyses of the hind paws showed better improvement in the AG4 group than in the SC and AG6 groups (Figure 4B).

#### Electrophysiological differences after grafting

Electrophysiological testing was performed at the end of the experiments in the AG4 and AG6 groups (Figure 5A and B). The MEP amplitude in the AG4 group (injured/uninjured ratio:  $73.1 \pm 4.7\%$ ) was significantly greater than that in the AG6 group ( $47.1 \pm 7.2\%$ ,  $P < 0.01$ ; Figure 5C). The MEP latency in the AG4 group ( $130.4 \pm 1.9\%$ ) was significantly lower than that in the AG6 group ( $147.7 \pm 5.7\%$ ) ( $P < 0.05$ ; Figure 5D). The higher MEP amplitude and faster conduction in the AG4 group indicated enhanced functional recovery of the reconstructed peroneal nerve compared to that in the AG6 group.

#### Discussion

We demonstrated that nerve repair at 4 weeks led to more successful recovery than that at 6 weeks after PNI in mice. The number of remaining NMJs in the denervated muscles was a key factor for functional recovery.

Atrophy occurs in the target muscles when reinnervation is delayed after PNI. The denervated muscles show irreversible changes if nerve repair is not performed in a timely manner. In general, peripheral nerves show better regeneration than central nerves after injury. Schwann cell responses after PNI are known to support nerve regeneration (Jessen and Mirsky, 2019). However, the molecular mechanisms of degeneration and regeneration are unclear in the chronic phase after PNI (Scheib and Höke, 2013). We showed that the number of  $\alpha$ -BTX-positive clusters was maintained until 4 weeks and then suddenly decreased from 6 weeks after peroneal nerve transection in mice. This degeneration pattern of NMJs until 8 weeks was consistent with a previous rat study (Andreose et al., 1995). Notably, the proportion of  $\alpha$ -BTX-positive clusters with pretzel morphology was equal to that of clusters with plaque morphology at 6 weeks after transection. Maintenance of the pretzel-type mature form indicates sufficient NMJ neurotransmission (Li et al., 2018). Thus, the prevention of NMJ degeneration around 6 weeks after PNI likely enhanced the regeneration capacity of the delayed peripheral nerve repair in the present study. Prolonged denervation is also associated with decreased trophic support from Schwann cells (Höke et al., 2002) and impaired maintenance of NMJs (Barik et al., 2016). The remaining

Schwann cells in the denervated muscles are thus an important factor for regeneration. We observed a stepwise decline of the number of Schwann cells in the TA muscles, coincident with irreversible changes of motor function. The significant change in the amount of Schwann cells between 4 and 6 weeks was consistent with the change in the number of NMJs in the present study. Thus, a sufficient amount of Schwann cells earlier than 6 weeks after PNI likely further supported the observed axonal regeneration upon delayed peripheral nerve repair.

There are methodological limitations in the present study. This regeneration process was unusual because the distal end of the donor nerve was directly connected to the denervated TA muscles. In the next opportunity, we will try to perform end-to-end repair of the distal stump at chronic phase and compare different surgical repair procedures. It will be technically overcome by leaving a knot in the distal stump of the peroneal nerve after transection. It should be noted that although we did not use such methods in the present study, 3D whole-tissue quantitative analyses of NMJs have recently been developed. In particular, new tissue clearing methods have been developed with various clearing agents (Zhu et al., 2013), and whole skeletal muscles have been cleared and presented as a 3D view of all NMJs stained with bungarotoxin (Williams et al., 2019). Future studies should utilize these methods to better determine the exact degeneration or regeneration pattern of NMJs and Schwann cells in the muscles.

Our findings suggest that in the clinic, it might be necessary to identify the critical time point for nerve reconstruction after PNI. The nerve reconstruction model in the present study is technically simple. The donor peroneal nerve was sutured to the proximal stump and then the distal end of the donor nerve was just inserted into the TA muscle layer. The effect of the distal stump of the peroneal nerve on nerve regeneration was thus eliminated. Schwann cells from the donor nerve were expected to provide presynaptic support for axonal regeneration. Ectopic NMJs far from the original innervation have been observed on denervated muscles, and postsynaptic differentiation occurred similarly to that of the original NMJs (Mathiesen et al., 1999). There are several potential reasons for the better recovery in the group grafted at 4 weeks after transection compared to the group grafted at 6 weeks. First, we considered whether the regenerated axons reached the muscle faster. However, YFP-positive axons had already reached the distal stump by 4 weeks after grafting in both groups. These results indicate that the regenerated axons at least reached the entry zone of the target muscle, facilitated by Schwann cells from the C57BL/6J allograft. Second, we considered whether the remaining Schwann cells or NMJs supported the regenerating axons in the denervated muscles. The number of Schwann cells decreased to less than 50% of that in the naïve mice, whereas the number of NMJs remained equal to that in the naïve mice at 4 weeks after transection. Recently, a chemokine from perisynaptic Schwann cells was shown to promote axonal regeneration, resulting in functional recovery (Negro et al., 2017). As shown in Fig. 3D, the number of Schwann cells increased by 4 weeks after grafting in both groups. During this time,

Schwann cells might have migrated from the donor nerves to the muscles, after which the presynaptic Schwann cells may have supported further axonal elongation, resulting in functional recovery. A previous rat study also showed that denervation less than 4 weeks after peroneal nerve transection did not affect axonal regeneration (Sulaiman and Gordon, 2000). It is thus likely that presynaptic Schwann cells play an important role in promoting further regeneration in the chronic phase after PNI. Finally, we considered whether the synaptic connections were different between the groups grafted at 4 and 6 weeks. There was no difference in innervation between the experimental groups, but a higher number of NMJs with pretzel morphology was observed with grafting at 4 weeks after transection than when grafting was performed at 6 weeks. Target muscles with a higher proportion of pretzel-shaped NMJs showed functional restoration in a study of embryonic motoneuron transplantation into the sciatic nerve (Kurimoto et al., 2016). A study of tourniquet-induced extremity injury also showed that disruption of the AChRs distribution dampened NMJ transmission and delayed functional recovery (Tu et al., 2017). Therefore, maintenance of pretzel-shaped NMJs during axonal regeneration likely enables efficient neurotransmission and enhances functional recovery after nerve repair. Interestingly, the PFI value in the AG6 group suddenly decreased at 8 weeks after grafting. Schwann cells from the donor nerves may have supported axonal elongation after grafting and maintained motor functions with growth factors. However, further degeneration of NMJs may have occurred during the regeneration, resulting in a loss of the motor endplates. Schwann cells also would have lost their targets and growth factor effects. The lower amount of surviving NMJs and Schwann cells in the AG6 group than in the AG4 group likely contributed to the drastic decrease in the PFI value.

Furthermore, molecular alterations occur in the denervated muscle from 4 to 6 weeks after PNI. In particular, agrin induces AChR clustering (Wu et al., 2010). We found no statistically significant differences in agrin mRNA expression in the denervated muscles between 4 and 6 weeks after transection (data not shown). Other mechanisms such as Dok-7 (Okada et al., 2006) or wnt signaling (Shen et al., 2018) may be involved in the degeneration or regeneration of NMJs after PNI. Further analyses of synaptic signaling and remodeling in NMJs are necessary.

In conclusion, we observed more NMJs in the target muscles and better functional recovery in the mice when nerve grafting was performed at 4 weeks than at 6 weeks after PNI. Our data suggest that remnant NMJs may facilitate nerve regeneration in denervated muscles in the chronic phase after PNI. At this time, it is difficult to noninvasively measure the number of AChRs or presynaptic Schwann cells in denervated muscles after PNI. Further studies using new detection modalities such as *in vivo* imaging may help to identify effective treatments.

**Acknowledgments:** We thank Dr. Shinichi Sotome of Tokyo Medical and Dental University for helpful discussions and Mrs. Tomoe Hori and Ms. Miyoko Ojima of Tokyo Medical and Dental University for technical assistance.

**Author contributions:** LL, ME and YW conceived and designed the

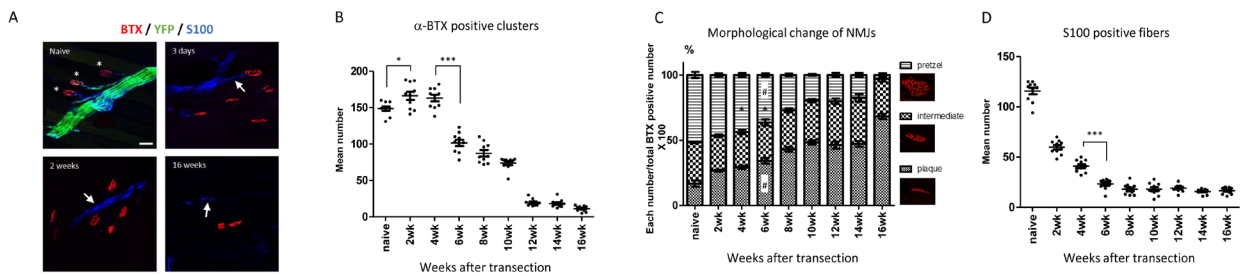


**Figure 1** Immunohistochemical staining and quantitative analyses of the tibialis anterior muscle following transection of the peroneal nerve in YFP mice.

(A) YFP-expressing axons (green) colabeled with S100-positive fibers (blue) were clearly observed in the tibialis anterior muscle, and their branches reached acetylcholine receptors labeled with  $\alpha$ -BTX (asterisks, red) in naïve mice. YFP-positive axons disappeared by 3 days, whereas S100-positive fibers (arrows, blue) and  $\alpha$ -BTX-positive clusters (red) remained even until 16 weeks after transection. Scale bar: 30  $\mu$ m. (B) The number of  $\alpha$ -BTX-positive clusters was increased at 2 weeks and then decreased from 6 weeks after transection. The experiments were repeated five times. (C) The number of pretzel-shaped  $\alpha$ -BTX-positive clusters decreased and that of plaques increased after transection. The proportion of the pretzel type at 4 weeks was significantly higher than that at 6 weeks (\*). There was no difference in the proportions of the pretzel and plaque types at 6 weeks (#). Representative morphologies of neuromuscular junction were shown in the graph legend. (D) The number of S100-positive fibers immediately decreased after transection and reached a plateau from 6 weeks after transection. Mean  $\pm$  SEM, \* $P$  < 0.05, \*\* $P$  < 0.001, one-way analysis of variance followed by Tukey's *post hoc* test (B and D), two-way analysis of variance followed by Bonferroni *post hoc* test (C). BTX: Bungarotoxin; YFP: yellow fluorescent protein.

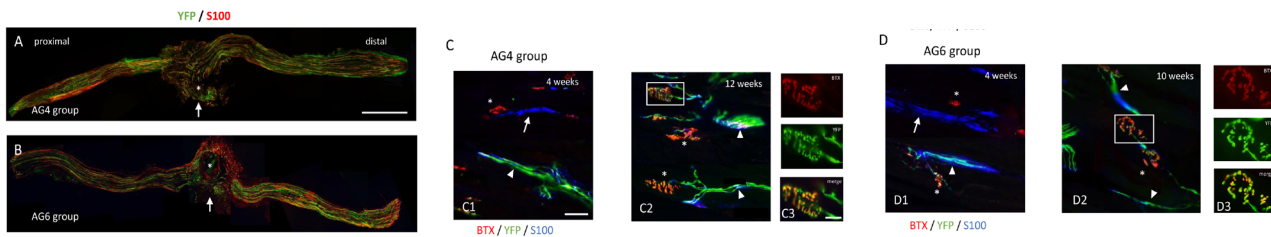


**Figure 2** Histological analyses in the reconstructed peroneal nerve and TA muscle after grafting.

(A, B) YFP-expressing axons (green) extended beyond the sutured site (arrows), and S100-positive fibers (red) were observed in longitudinal sections of the peroneal nerve 4 weeks after grafting in the AG4 and AG6 groups. The hole of the surgical suture is shown with an asterisk in A and B. (C) These images were obtained from the TA muscle at 4 (C1) and 12 weeks (C2) after grafting. AChRs were labeled with  $\alpha$ -BTX (red). Thick YFP-expressing axons (green) colabeled with S100-positive fibers (blue) were observed with branches (arrowheads in C1 and C2). Pretzel-shaped AChR distributions (asterisk in C1) were observed near S100-positive fibers (arrow in C1). Mature AChRs (asterisks in C2) were observed at 12 weeks. Within the square shown in C2, the AChR-expressing cluster was innervated by YFP-expressing axons (C3). (D) These images were obtained from the TA muscle at 4 (D1) and 10 weeks (D2) after grafting. YFP-expressing axons colabeled with S100-positive fibers were observed with fewer branches (arrowheads in D1 and D2). The intermediate type of AChR distribution (asterisk in D1) was observed near S100-positive fibers (arrow in D1). Pretzel-shaped AChR distributions (asterisks in D2) were observed at 10 weeks. Fragmentation of AChRs was observed in the square shown in D2 (D3). Scale bars: 500  $\mu$ m (A and B), 50  $\mu$ m (C1, C2 and D1, D2), 20  $\mu$ m (C3 and D3). AChR: Acetylcholine receptor; BTX: bungarotoxin; TA: tibialis anterior; YFP: yellow fluorescent protein. AG4 and AG6: Allograft transplantation at 4 and 6 weeks after injury.

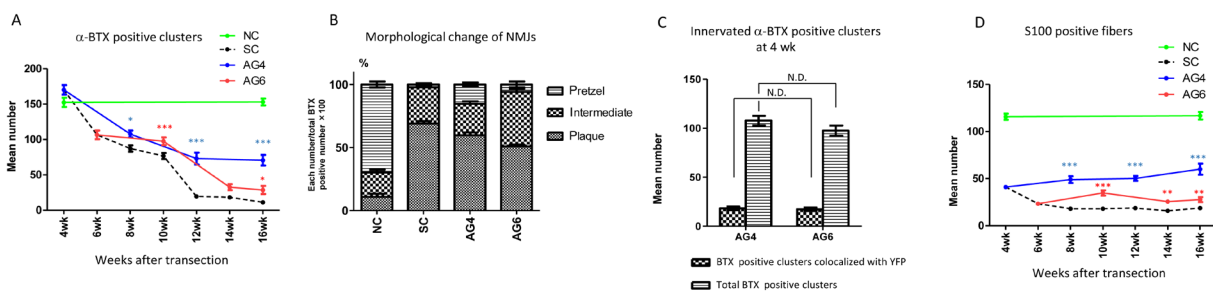


**Figure 3** Quantitative analyses of NMJs and Schwann cells in TA muscle after grafting.

(A) Higher numbers of  $\alpha$ -BTX-positive clusters were observed 4 weeks after grafting in both the AG4 (blue line, asterisk) and AG6 groups (red line, three asterisks) than in the SC group (black dotted line). The number at the final observation point was significantly increased in the AG4 group (blue line, three asterisks). The experiments were repeated five times. (B) The morphological changes of NMJs were evaluated at the final observation point. More pretzel-shaped NMJs were observed in the AG4 group than in the other groups. (C) There was no difference in innervated  $\alpha$ -BTX-positive clusters between the AG4 and AG6 groups at 4 weeks after grafting. (D) More S100-positive cells were observed 4 weeks after grafting in both the AG4 (blue line, three asterisks) and AG6 groups (red line, three asterisks) than in the SC group. The number of S100-positive cells at the final observation point was significantly increased in the AG4 group (three asterisks). Mean  $\pm$  SEM, \* $P$  < 0.05, \*\* $P$  < 0.01, \*\*\* $P$  < 0.001, two-way analysis of variance followed by Bonferroni *post hoc* test (A, B and D). Unpaired two-tailed Student's *t*-test (C). BTX: Bungarotoxin; N.D.: No differences; NMJ: neuromuscular junction; TA: tibialis anterior. NC: naïve control group; SC: surgical control group; AG4 and AG6: allograft transplantation at 4 and 6 weeks after injury.

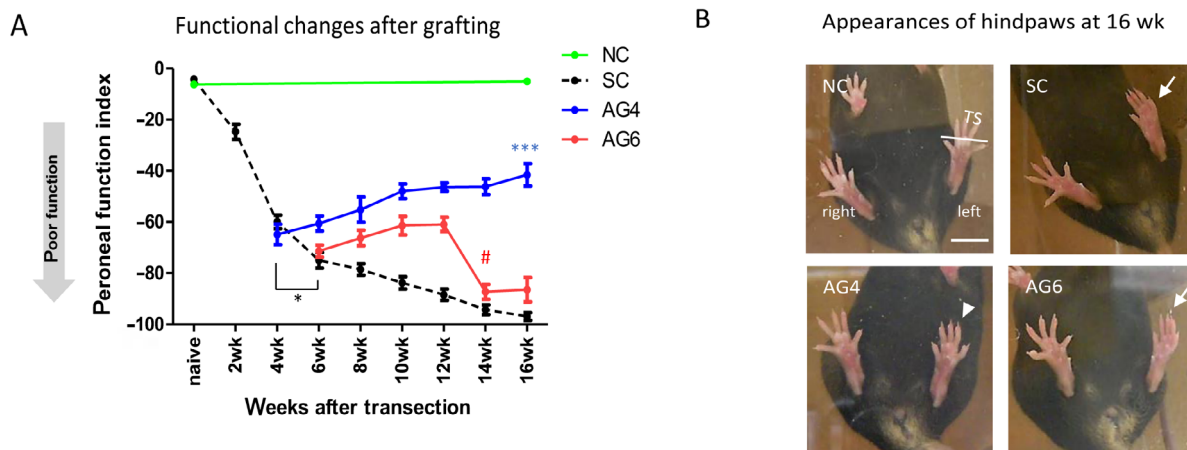


**Figure 4 Functional recovery of the hindpaw after transection and reconstruction with a nerve graft.**

(A) PFI values, an indicator of functional recovery, immediately decreased after transection (black dotted line). PFI values were significantly different between 4 and 6 weeks after transection ( $*P < 0.05$ ). After grafting, the PFI values increased in both the AG4 (blue line) and AG6 (red line) groups, but they decreased at 8 weeks in the AG6 group (#). The AG4 group had higher PFI values than the other groups at the final observation point ( $***P < 0.001$ ). The experiments were repeated five times. Mean  $\pm$  SEM,  $*P < 0.05$ ,  $***P < 0.001$ , two-way analysis of variance followed by Bonferroni *post hoc* test. (B) Hindpaw images were obtained from video analyses at the final observation point. Narrowing of the toe spread (TS) was observed in the SC and AG6 groups (arrows) but not in the AG4 group (arrow head). Scale bar: 10 mm. PFI: Peroneal nerve function index. NC: naïve control group; SC: surgical control group; AG4 and AG6: allograft transplantation at 4 and 6 weeks after injury.

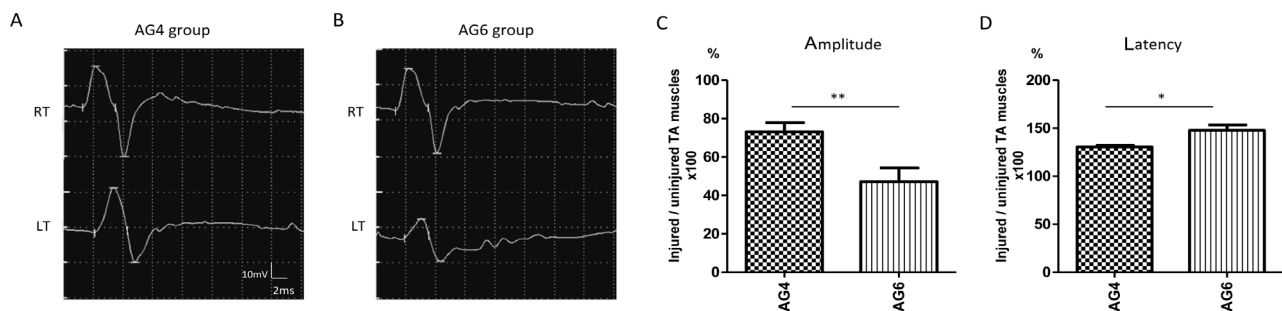


**Figure 5 Electrophysiological assessment of the TA muscle in the AG4 and AG6 groups at the final observation point.**

(A, B) Representative MEPs were obtained from both hindlimbs (RT: intact side, LT: grafted side). The MEP recorded from the LT had an obviously low amplitude in the AG6 group. MEP amplitudes and latencies were measured in both hindlimbs and then the injured/uninjured ratio was calculated. (C) The AG4 group displayed greater MEP amplitudes than the AG6 group. (D) The AG4 group also displayed shorter MEP latencies than the AG6 group. The experiments were repeated five times. Mean  $\pm$  SEM,  $*P < 0.05$ ,  $**P < 0.01$ . Unpaired two-tailed Student's *t*-test (C and D). MEP: Muscle evoked potential; TA: tibialis anterior. AG4 and AG6: allograft transplantation at 4 and 6 weeks after injury.

**Table 1 Diagram of histological and electrophysiological evaluations of the tibialis anterior muscle in the experimental groups**

Experimental group	Time course										
	0 wk	2 wk	4 wk	6 wk	8 wk	10 wk	12 wk	14 wk	16 wk		
Naïve control (NC) group	Intact histology	[Green bar]									
Surgical control (SC) group		histology	histology	histology	histology	histology	histology			Histology	
Allograft at 4 weeks after transection (AG4) group	Left peroneal nerve transection		allograft	histology						Electrophysiological test in the AG4 and AG6 groups	
Allograft at 6 weeks after transection (AG6) group			allograft	histology							

study and wrote the manuscript. LL, ME, HY, HK, TH and KT collected the data, performed the experiments, and analyzed the data. LL, ME, YW and AO interpreted results of experiments. HY, HK, TH, KT, YW and AO revised the manuscript. All authors read and accepted the final version of the manuscript submitted for publication.

**Conflicts of interest:** None of the authors has any commercial association that might pose or create a conflict of interest with information presented in this article.

**Financial support:** This work was supported by the Japan Society for the Promotion of Science KAKENHI (Grants 26462230 and 16K10813) and grants from the Japan Student Services Organization (JASSO).

**Institutional review board statement:** All animal experiments were approved by the Institutional Animal Care and Use Committee of Tokyo Medical and Dental University on 5 July 2017, 30 March 2018, and 15 May 2019 (A2017-311C, A2018-297A, and A2019-248A), respectively.

**Copyright license agreement:** The Copyright License Agreement has been signed by all authors before publication.

**Data sharing statement:** Datasets analyzed during the current study are available from the corresponding author on reasonable request.

**Plagiarism check:** Checked twice by iThenticate.

**Peer review:** Externally peer reviewed.

**Open access statement:** This is an open access journal, and articles are distributed under the terms of the Creative Commons Attribution-NonCommercial-ShareAlike 4.0 License, which allows others to remix, tweak, and build upon the work non-commercially, as long as appropriate credit is given and the new creations are licensed under the identical terms.

**Open peer reviewers:** Fei Yu, Peking University Shenzhen Hospital, China; Fei Ding, Affiliated Hospital of Nantong University, China.

**Additional file:** Open peer review reports 1 and 2.

## References

- Andreose JS, Fumagalli G, Lomo T (1995) Number of junctional acetylcholine receptors: control by neural and muscular influences in the rat. *J Physiol* 483(Pt 2):397-406.
- Ashley Z, Sutherland H, Lanmüller H, Russold MF, Unger E, Bijak M, Mayr W, Boncompagni S, Protasi F, Salmons S, Jarvis JC (2007) Atrophy, but not necrosis, in rabbit skeletal muscle denervated for periods up to one year. *Am J Physiol Cell Physiol* 292:C440-451.
- Bain JR, Mackinnon SE, Hunter DA (1989) Functional evaluation of complete sciatic, peroneal, and posterior tibial nerve lesions in the rat. *Plast Reconstr Surg* 83:129-138.
- Barik A, Li L, Sathyamurthy A, Xiong WC, Mei L (2016) Schwann Cells in Neuromuscular Junction Formation and Maintenance. *J Neurosci* 36:9770-9781.
- Bervar M (2000) Video analysis of standing--an alternative footprint analysis to assess functional loss following injury to the rat sciatic nerve. *J Neurosci Methods* 102:109-116.
- Birks R, Katz B, Miledi R (1960) Physiological and structural changes at the amphibian myoneural junction, in the course of nerve degeneration. *J Physiol* 150:45-168.
- Chao T, Frump D, Lin M, Caiozzo VJ, Mozaffar T, Steward O, Gupta R (2013) Matrix metalloproteinase 3 deletion preserves denervated motor endplates after traumatic nerve injury. *Ann Neurol* 73:210-223.
- de Medinaceli L, Freed WJ, Wyatt RJ (1982) An index of the functional condition of rat sciatic nerve based on measurements made from walking tracks. *Exp Neurol* 77:634-643.
- Feng G, Mellor RH, Bernstein M, Keller-Peck C, Nguyen QT, Wallace M, Nerbonne JM, Lichtman JW, Sanes JR (2000) Imaging neuronal subsets in transgenic mice expressing multiple spectral variants of GFP. *Neuron* 28:41-51.
- Fu SY, Gordon T (1995a) Contributing factors to poor functional recovery after delayed nerve repair: prolonged axotomy. *J Neurosci* 15:3876-3885.
- Fu SY, Gordon T (1995b) Contributing factors to poor functional recovery after delayed nerve repair: prolonged denervation. *J Neurosci* 15:3886-3895.
- Höke A, Gordon T, Zochodne DW, Sulaiman OA (2002) A decline in glial cell-line-derived neurotrophic factor expression is associated with impaired regeneration after long-term Schwann cell denervation. *Exp Neurol* 173:77-85.
- Inserra MM, Bloch DA, Terris DJ (1998) Functional indices for sciatic, peroneal, and posterior tibial nerve lesions in the mouse. *Microsurgery* 18:119-124.
- Jessen KR, Mirsky R (2019) The success and failure of the Schwann cell response to nerve injury. *Front Cell Neurosci* 13:33.
- Jivan S, Kumar N, Wiberg M, Kay S (2009) The influence of pre-surgical delay on functional outcome after reconstruction of brachial plexus injuries. *J Plast Reconstr Aesthet Surg* 62:472-479.
- Jonsson S, Wiberg R, McGrath AM, Novikov LN, Wiberg M, Novikova LN, Kingham PJ (2013) Effect of delayed peripheral nerve repair on nerve regeneration, Schwann cell function and target muscle recovery. *PLoS One* 8:e56484.
- Keller-Peck CR, Feng G, Sanes JR, Yan Q, Lichtman JW, Snider WD (2001) Glial cell line-derived neurotrophic factor administration in postnatal life results in motor unit enlargement and continuous synaptic remodeling at the neuromuscular junction. *J Neurosci* 21:6136-6146.
- Kummer TT, Misgeld T, Lichtman JW, Sanes JR (2004) Nerve-independent formation of a topologically complex postsynaptic apparatus. *J Cell Biol* 164:1077-1087.
- Kurimoto S, Kato S, Nakano T, Yamamoto M, Takanobu N, Hirata H (2016) Transplantation of embryonic motor neurons into peripheral nerve combined with functional electrical stimulation restores functional muscle activity in the rat sciatic nerve transection model. *J Tissue Eng Regen Med* 10:E477-484.
- Li L, Xiong WC, Mei L (2018) Neuromuscular junction formation, aging, and disorders. *Annu Rev Physiol* 80:159-188.
- Lin W, Burgess RW, Dominguez B, Pfaff SL, Sanes JR, Lee KF (2001) Distinct roles of nerve and muscle in postsynaptic differentiation of the neuromuscular synapse. *Nature* 410:1057-1064.
- Ma CH, Omura T, Cobos EJ, Latrémolière A, Ghasemlou N, Brenner GJ, van Veen E, Barrett L, Sawada T, Gao F, Coppola G, Gertler F, Costigan M, Geschwind D, Woolf CJ (2011) Accelerating axonal growth promotes motor recovery after peripheral nerve injury in mice. *J Clin Invest* 121:4332-4347.
- Marques MJ, Conchello JA, Lichtman JW (2000) From plaque to pretzel: fold formation and acetylcholine receptor loss at the developing neuromuscular junction. *J Neurosci* 20:3663-3675.
- Mathiesen I, Rimer M, Ashtari O, Cohen I, McMahan UJ, Lomo T (1999) Regulation of the size and distribution of agrin-induced postsynaptic-like apparatus in adult skeletal muscle by electrical muscle activity. *Mol Cell Neurosci* 13:207-217.
- Millesi H (2000) Techniques for nerve grafting. *Hand Clin* 16:73-91, viii.
- Negro S, Lessi F, Duregotti E, Aretini P, La Ferla M, Franceschi S, Menicagli M, Bergamin E, Radice E, Thelen M, Megighian A, Pirazzini M, Mazzanti CM, Rigoni M, Montecucco C (2017) CXCL12 $\alpha$ /SDF-1 from perisynaptic Schwann cells promotes regeneration of injured motor axon terminals. *EMBO Mol Med* 9:1000-1010.
- Okada K, Inoue A, Okada M, Murata Y, Kakuta S, Jigami T, Kubo S, Shiraishi H, Eguchi K, Motomura M, Akiyama T, Iwakura Y, Higuchi O, Yamanashi Y (2006) The muscle protein Dok-7 is essential for neuromuscular synaptogenesis. *Science* 312:1802-1805.
- Rosenfield J, Paksima N (2001) Peripheral nerve injuries and repair in the upper extremity. *Bull Hosp Jt Dis* 60:155-161.
- Sakuma M, Gorski G, Sheu SH, Lee S, Barrett LB, Singh B, Omura T, Latrémolière A, Woolf CJ (2016) Lack of motor recovery after prolonged denervation of the neuromuscular junction is not due to regenerative failure. *Eur J Neurosci* 43:451-462.
- Scheib J, Höke A (2013) Advances in peripheral nerve regeneration. *Nat Rev Neurol* 9:668-676.
- Shen C, Li L, Zhao K, Bai L, Wang A, Shu X, Xiao Y, Zhang J, Zhang K, Hui T, Chen W, Zhang B, Hsu W, Xiong WC, Mei L (2018) Motoneuron Wnts regulate neuromuscular junction development. *Elife* 7.
- Shi L, Butt B, Ip FC, Dai Y, Jiang L, Yung WH, Greenberg ME, Fu AK, Ip NY (2010) Ephexin1 is required for structural maturation and neurotransmission at the neuromuscular junction. *Neuron* 65:204-216.
- Sulaiman OA, Gordon T (2000) Effects of short- and long-term Schwann cell denervation on peripheral nerve regeneration, myelination, and size. *Glia* 32:234-246.
- Susarla SM, Kaban LB, Donoff RB, Dodson TB (2007) Does early repair of lingual nerve injuries improve functional sensory recovery? *J Oral Maxillofac Surg* 65:1070-1076.
- Tu H, Zhang D, Corrick RM, Muelleman RL, Wadman MC, Li YL (2017) Morphological regeneration and functional recovery of neuromuscular junctions after tourniquet-induced injuries in mouse hindlimb. *Front Physiol* 8:207.
- Webb CM, Cameron EM, Sundberg JP (2012) Fluorescence-labeled reporter gene in transgenic mice provides a useful tool for investigating cutaneous innervation. *Vet Pathol* 49:727-730.
- Williams MPI, Rigon M, Straka T, Hörner SJ, Thiel M, Gretz N, Hafner M, Reischl M, Rudolf R (2019) A novel optical tissue clearing protocol for mouse skeletal muscle to visualize endplates in their tissue context. *Front Cell Neurosci* 13:49.
- Wu H, Xiong WC, Mei L (2010) To build a synapse: signaling pathways in neuromuscular junction assembly. *Development* 137:1017-1033.
- Yan Y, Sun HH, Mackinnon SE, Johnson PJ (2011) Evaluation of peripheral nerve regeneration via in vivo serial transcutaneous imaging using transgenic Thy1-YFP mice. *Exp Neurol* 232:7-14.
- Zhu D, Larin KV, Luo Q, Tuchin VV (2013) Recent progress in tissue optical clearing. *Laser Photon Rev* 7:732-757.

P-Reviewers: Yu F, Ding F; C-Editors: Zhao M, Li CH; T-Editor: Jia Y